ABSTRACT

Modal parameters obtained from modal testing (such as modal vectors, natural frequencies, and damping ratios) have been used extensively in system identification, finite element model updating, and structural health monitoring. As an alternative to modal vectors, load-dependent Ritz vectors have been shown useful in various areas of structural dynamics such as model reduction and damage detection. The applications of Ritz vectors, however, have been mainly limited in analytical and numerical analyses because of the difficulty to identify them from vibration tests. This paper presents a procedure to extract load-dependent Ritz vectors using a flexibility matrix constructed from measured vibration test data. The proposed method can not only construct the Ritz vectors corresponding to the actual load pattern employed in vibration tests, but also generate Ritz vectors from arbitrary load patterns. Experimental test data obtained from a grid-type bridge structure are employed to validate and illustrate the proposed extraction procedure.

INTRODUCTION

Modal parameters such as modal vectors, natural frequencies, and damping have been widely employed in many fields of structural dynamics. For example, in numerical dynamic analysis, a multi-degree-of-freedom (MDOF) system can be decoupled into a number of single-degree-of-freedom (SDOF) systems using the orthogonality feature of modal vectors and the vibration response of the system can be approximated by the superposition of a small set of the SDOF system responses. For vibration test, the response time histories are typically transformed into the frequency domain using a spectral analyzer and the test results are often presented in the form of modal parameters.

It has been shown that load-dependent Ritz vectors have many potential

[*]Postdoctoral Research Fellow, Engineering Sciences and Applications Division, Engineering Analysis Group, Los Alamos National Laboratory, Los Alamos, NM 87545

[†]Department of Civil and Environmental Engineering, Stanford University, Stanford, CA94305-4020

advantages in structural dynamics over modal parameters. For linear dynamic analyses, the response quantities of interest can be approximated more effectively by a smaller number of Ritz vectors than the modal vectors [8, 11]. In numerical analysis, Ritz (or Lanczos) vectors have been used to find partial extremal solutions of large eigenvalue problems [6] and to reanalyze a structural system with localized modifications [3]. In structural monitoring and damage diagnosis, numerical simulations have shown that Ritz vectors are able to identify damage better than modal vectors [1, 10]. For system identification and damage detection problems, however, the Ritz vectors need to be obtained from experimental test data.

Cao and Zimmerman [2] are probably the first to attempt extracting Ritz vectors from measured vibration data using a state-space formulation. In this paper, we present a new extraction procedure based on a flexibility matrix obtained from vibration test data. While the method proposed by Cao and Zimmerman constructs the Ritz vectors corresponding to the actual load pattern imposed on the structure, the proposed method is able to generate Ritz vectors from assumed load patterns as well. The effectiveness of the new extraction procedure is demonstrated using the data obtained from a vibration test of a grid-type bridge structure.

This paper is organized as follows: First, the proposed flexibility matrix based method is described. Next, we briefly describe the grid-type bridge model employed in the experimental study and the finite element model corresponding to the test structure. The proposed extraction procedure is then demonstrated and compared with the state-space based method using the experimental test data. Finally, this paper is concluded with a summary and discussions.

FLEXIBILITY BASED EXTRACTION OF RITZ VECTORS

Cao and Zimmerman [2] proposed a procedure to extract Ritz vectors based on the state-space matrices estimated from vibration tests. In this section, we present a new extraction procedure of Ritz vectors based on a measured flexibility matrix. A close look at the analytical generation procedure in Reference [2] reveals that the generation of Ritz vectors uses the flexibility matrix $\mathbf{F}$ (defined here as the inverse of the stiffness matrix) rather than the stiffness matrix itself.

The extraction of Ritz vectors starts with the assumption that the dynamic loading $\mathbf{F}(t)$ can be separated into a spatial load vector $\mathbf{f}$ and time function $u(t)$:

$$\mathbf{F}(t) = \mathbf{f}u(t) \tag{1}$$

If the modal vectors are mass-normalized such that

$$\begin{aligned} \mathbf{V}^T\mathbf{K}\mathbf{V} &= \Omega \\ \mathbf{V}^T\mathbf{M}\mathbf{V} &= \mathbf{I} \end{aligned} \tag{2}$$

the flexibility matrix then can be represented with the modal parameters [4]:

$$\mathbf{F} = \mathbf{K}^{-1} = \mathbf{V}\Omega^{-1}\mathbf{V}^T \tag{3}$$

where Ω is the diagonal eigenvalue matrix and $\mathbf{V}$ is the corresponding eigenvector (modal vector) matrix. In most experimental modal analyses, only a few lower modal frequencies and modal vectors are identified. For this case, the flexibility matrix is divided into the *modal flexibility*, which is formed from the estimated frequencies and modal vectors, and the *residual flexibility* formed from the residual modes [4]:

$$\mathbf{F} = \mathbf{F}_m + \mathbf{F}_r = \mathbf{V}_m \Omega_m^{-1} \mathbf{V}_m^T + \mathbf{V}_r \Omega_r^{-1} \mathbf{V}_r^T \tag{4}$$

where the subscript m and r denote the estimated and residual quantities, respectively. Here, the modal flexibility matrix is constructed only from the measured natural frequencies and modal vectors ($\mathbf{F}_m = \mathbf{V}_m \Omega_m^{-1} \mathbf{V}_m^T$). The residual flexibility is the contribution of the unmeasured dynamic modes to the full flexibility matrix. Note that the contribution of lower modes, which are normally estimated in experimental modal analyses, are more significant than those of higher modes because the contribution of each mode is inversely proportional to the magnitude of the corresponding natural frequencies.

From the modal flexibility matrix $\mathbf{F}_m$ and the analytical mass matrix $\mathbf{M}$, the first Ritz vector can be computed as:

$$\bar{\mathbf{r}}_1 = \mathbf{F}_m \mathbf{f} \tag{5}$$

where $\mathbf{f}$ is the spatial load distribution vector defined in Equation (1). The first Ritz vector is, then, mass-normalized as:

$$\mathbf{r}_1 = \frac{\tilde{\mathbf{r}}_1}{[\tilde{\mathbf{r}}_1^T \mathbf{M} \tilde{\mathbf{r}}_1]^{\frac{1}{2}}} \tag{6}$$

The following Ritz vectors are recursively generated. Assuming the mass matrix times the previous Ritz vector $\mathbf{M}\mathbf{r}_{s-1}$ as a load, the recurrence relationship computes the next Ritz vector $\bar{\mathbf{r}}_s$:

$$\bar{\mathbf{r}}_s = \mathbf{F}_m \mathbf{M} \mathbf{r}_{s-1} \tag{7}$$

The linear independence of Ritz vectors is achieved using the Gram-Schmidt orthogonalization:

$$\tilde{\mathbf{r}}_s = \bar{\mathbf{r}}_s - \sum_{t=1}^{s-1} (\mathbf{r}_t^T \mathbf{M} \bar{\mathbf{r}}_s) \mathbf{r}_t \tag{8}$$

Finally, the current Ritz vector is mass-normalized:

$$\mathbf{r}_s = \frac{\tilde{\mathbf{r}}_s}{[\tilde{\mathbf{r}}_s^T \mathbf{M} \tilde{\mathbf{r}}_s]^{\frac{1}{2}}} \tag{9}$$

It is worthwhile to compare the flexibility based extraction procedure with the state-space based procedure proposed by Cao and Zimmerman [2]. Since the spatial load distribution vector $\mathbf{f}$ in Equation (5) can be assigned arbitrary, the flexibility based method is able to generate different sets of Ritz vectors.

On the other hand, the state-space matrices estimated from the experimental modal analysis retains the information of the actual load pattern used in the modal test. Therefore, the state-space based method only identifies the Ritz vectors corresponding to the specific excitation pattern used in the actual modal testing. Note that both methods require an appropriate approximation for the mass matrix. However, since stiffness changes are the main concern of damage detection, the exact estimation of the mass matrix is not necessary.

AN EXPERIMENTAL BRIDGE MODEL

For this study, a grid-type bridge model has been constructed and tested at the Hyundai Institute of Construction Technology (HICT), Korea (Figure 1). The steel bridge model consists of two parallel girders and six evenly spaced cross beams connecting the two girders. The girders are steel rectangular tubes and the cross beams are C-shape members. Using impact excitations, we extract Ritz and modal vectors from the vibration response of this test structure.

A SA-390 signal analyzer with four channels is used for the analog to digital conversion of accelerometer signals and the Fast Fourier Transform (FFT) calculation. Data acquisition parameters are specified such that a frequency response function (FRF) in the range of 0 to 100 Hz could be estimated. Each spectrum is computed by averaging three 8 seconds long time histories. A total of 2048 points are sampled for a 8 second time period and this sampling rate produces a frequency resolution of 0.125 Hz. An exponential window is applied to all measured time histories prior to the FFT calculation.

For measurements, a Dytran 5801A4 impact hammer and three Dytran 3100B accelerometers with a normal sensitivity of 100 mV/g are used. The excitation is applied at nodes 3, 4 and 5 as shown in Figure 2. The sensors measure the vertical accelerations at the twelve nodes as indicated in Figure 2. Note that since the SA-390 data acquisition system has only four channels and there are three accelerometers, the first channel is always connected to the input hammer and the remaining three channels are connected to three accelerometers. To complete one set of modal test, the hammer excitation is repeated twelve times at one point and the three accelerometers are moved from one set of three nodes to another set of three nodes after every three excitations. Note that each FRF is computed by averaging the three response time histories, and there are twelve measurement points and three accelerometers. The rational polynomial [9] techniques are employed to extract the first six natural frequencies and the corresponding modal vectors from the recorded FRFs.

ANALYTICAL MODELING OF THE TEST STRUCTURE

A finite element (FE) model for the grid type bridge structure is constructed using twenty three-dimensional beam elements. As shown in Figure 2, a girder segment between two nodes or a cross beam is modeled as a single element. An elastic modulus of 2.0×10^5 MPa, a mass density of 7850 kg/m^3, and a Poission ratio of 0.2 are specified for the model. Since the accelerometers measure only the vertical movement of the structure, the lateral DOFs are not included in the analytical model. Therefore, each node of an element has two translational DOFs and three rotational DOFs. The model has a total of 64 DOFs including four rotational DOFs at the boundary. Both ends of the beam are modeled as simple pinned connections. A pinned connection is modeled by a ball bearing with a 35 mm diameter in the experimental setup. Based on a preliminary vibration test, the boundary conditions appear to be less accurately modeled. The boundary conditions are then modified by introducing rotational springs at the rotational DOFs of the boundaries. Furthermore, additional springs are added to the rotational DOFs at both ends of the cross beams to simulate the bolted connection between the girders and the cross beams. After these modifications, the relative errors of the first six natural frequencies between the analytical model and the test structure fall within 4%.

Table 1 compares the natural frequencies of the analytical model computed after model updating with the experimental frequencies. Here, the experimental frequency ($\hat{\omega}$) is a mean value of the three frequencies estimated with an impact load applied at nodes 3, 4 and 5, respectively. Figure 3 displays the analytical and experimental modal vectors of the first six modes. All figures are plotted in the global X-Y plane of Figure 2, viewing the structure from the side.

As for the scaling of the modal or Ritz vectors, a mass-normalization is conducted. However, since the DOFs of the analytical model do not coincide with the DOFs of the experimental modal vectors, a reduced analytical mass matrix is first computed using the Guyan (static) condensation procedure [7]. Both the analytical and experimental vectors are normalized with respect to the reduced mass matrix. Errors arisen from the model reduction are found to be minimum since the inertial forces associated with the omitted rotational and axial DOFs (slave DOFs) are negligible in this example.

EXPERIMENTAL VERIFICATION

The experimental Ritz vectors are first computed following the state-space based procedure. Figure 4 compares the first six Ritz vectors estimated by the state-space method with the corresponding Ritz vectors computed from the FE model. The experimental Ritz vectors in Figure 4 are obtained with an impulse excitation at node 5. For the analytical procedure, a unit value is assigned to the vertical DOF of node 5 for the load pattern vector $\mathbf{f}$ in Equation (5). The first Ritz vector is equivalent to a deflection pattern observed when a unit load is applied at node 5. Figure 4 shows a good agreement between the experimental and analytical Ritz vecotrs. More quantitative analysis is presented in Table 2 where the Modal Assurance Criterion (MAC) values are defined as follows:

$$MAC(i,j) = \frac{(\mathbf{r}_i^T \mathbf{M} \hat{\mathbf{r}}_j)^2}{(\mathbf{r}_i^T \mathbf{M} \mathbf{r}_i)(\hat{\mathbf{r}}_j^T \mathbf{M} \hat{\mathbf{r}}_j)} \tag{10}$$

where $\mathbf{r}_i$ and $\hat{\mathbf{r}}_j$ are the analytical and experimental Ritz vectors, respectively.

The extraction of Ritz vectors is repeated using the flexibility matrix based method. Table 3 presents the comparison of MAC values between the analytical Ritz vectors and the ones computed using the measured flexibility matrix. Again, the Ritz vectors generated with a point load at node 5 are presented. The comparison of Tables 2 and 3 reveals that the state-space and flexibility based methods basically produce the same results. Although not presented, the Ritz vectors generated from the other two impulse excitations at nodes 3 and 4 by the two extraction procedures are practically identical.

As mentioned earlier, the flexibility matrix based method allows to generate Ritz vectors from any fictitious load patterns as well as the actual load pattern applied during the tests. In Table 4, the experimental Ritz vectors generated from an imaginary point load at nodes $2 \sim 7$ and $10 \sim 15$ are extracted and the MAC comparison with the corresponding analytical Ritz vectors are presented. For brevity, only the diagonal components of the MAC values are shown in the table. The result indicates that the Ritz vectors can be successfully generated from all the load patterns imposed. Next, imaginary point loads are simultaneously applied to nodes 2 and 5 (upward point load at node 2 and downward point load at node 5) and the corresponding Ritz vectors are generated. The Ritz vectors are plotted in Figure 5 and the MAC values are presented in Table 5.

SUMMARY AND DISCUSSIONS

In this paper, a new procedure has been proposed to extract load-dependent Ritz vectors from vibration test data. First, a flexibility matrix is approximated from measured modal vectors and natural frequencies. Then, Ritz vectors are recursively generated using the measured flexibility matrix. The procedure is successfully demonstrated using an experiment of a grid-type bridge structure and the performance of the proposed method is compared with that of the state-space based method [2]. The proposed method has at least two advantages over the state-space method: (1) The procedure is computationally more efficient requiring only the identification of classical modal vectors and natural frequencies, and (2) the proposed method is able to generate Ritz vectors from any arbitrary load patterns. Furthermore, the increased amount of information and better sensitivity to structural parameter changes, which are achievable by multiple loading and careful selection of load patterns, could improve the results of damage detection, model refinement, or component mode synthesis.

For the procedure described in this paper, only the modal flexibility is used for the computation of the measured flexibility matrix (see Equation (4)). Doebling et al. [5] have shown that a residual flexibility matrix with complete reciprocity can be estimated from experimental modal analyses. Using this technique, one can include the residual flexibility to compute the flexibility matrix. The inclusion of the residual flexibility matrix into the flexibility matrix should further allow the contribution of higher residual modes into experimentally estimated Ritz vectors.

ACKNOWLEDGMENTS

This work is supported by National Science Foundation under Grant No. CMS-95261-2. The authors wish to recognize the Hyundai Institute of Construction Technology (HICT), Korea for providing the laboratories and their personnel. The authors also would like to thank Mr. Jeong Hwan Jang of Seoul National University for his invaluable contributions to the experimental portion of this paper.

REFERENCES

[1] T. T. Cao and D. C. Zimmerman. Application of load-dependent Ritz vectors in structural damage detection. In *Proceedings of the 15th International Modal Analysis Conference*, pages 1319–1324, Orlando, FL, 1997.

[2] T. T. Cao and D. C. Zimmerman. A procedure to extract Ritz vectors from dynamic testing data. In *Proceedings of the 15th International Modal Analysis Conference*, pages 1036–1042, Orlando, FL, 1997.

[3] C. M. M. Carey, G. H. Colub, and K. H. Law. A Lanczos-based method for structural dynamic reanalysis problems. *International Journal for Numerical Methods in Engineering*, 37:2857–2883, 1994.

[4] S. W. Doebling. *Measurement of Structural Flexibility Matrices for Experiments with Incomplete Reciprocity.* PhD thesis, Aerospace Engineering Sciences, University of Colorado, Boulder, CO, 1995.

[5] S. W. Doebling, L. D. Peterson, and K. Alvin. Estimation of reciprocal residual flexibility from experimental modal data. *American Institute of Aeronautics and Astronautics*, 34:1678–1685, 1996.

[6] G. H. Golub and C. F. Van Loan. *Matrix Computations.* The Johns Hopkins University Press, Maryland, 1996.

[7] R. J. Guyan. Reduction of stiffness and mass matrices. *American Institute of Aeronautics and Astronautics*, 3:380, 1965.

[8] B. Nour-Omid and R. W. Clough. Dynamics analysis of structures using Lanczos coordinates. *Earthquake Engineering and Structural Dynamics*, 12:565–577, 1984.

[9] M. H. Richardson and D. L. Formenti. Parameter estimation form frequency response measurements using rational fraction polynomials. In *Proceedings of the the 1st International Modal Analysis Conference*, pages 167–181, Orlando, FL, 1982.

[10] H. Sohn and K. H. Law. Application of load-dependent Ritz vectors to Bayesian probabilistic damage detection. *Probabilistic Engineering Mechanics*, 1999. (in print).

[11] E. L. Wilson, M. W. Yuan, and J. M. Dicken. Dynamic analysis by direct superposition of Ritz vectors. *Earthquake Engineering and Structural Dynamics*, 10:813–821, 1982.

Table 1: Comparison of the analytical and experimental natural frequencies

Mode	Frequency (Hz) Analytical (ω)	Experimental ($\hat{\omega}$)	Relative Error* (%)
1st Bending	5.4488	5.5635	2.06
1st Torsion	10.1494	10.0406	1.08
2nd Bending	19.1841	18.6410	2.91
2nd Torsion	30.6216	29.4388	4.02
3rd Bending	41.6086	42.5910	2.31
3rd Torsion	54.9704	57.1864	3.88

* error=$|\omega - \hat{\omega}|/\hat{\omega}$

Table 2: MAC values between analytical and experimental Ritz vectors (using the state-space based method)

$MAC(i,j)^*$		$\hat{\mathbf{r}}_j$ 1	2	3	4	5	6
$\mathbf{r}_i$	1	0.9990	0.0001	0.0001	0.0000	0.0004	0.0001
	2	0.0001	0.9964	0.0004	0.0013	0.0002	0.0014
	3	0.0001	0.0006	0.9958	0.0009	0.0003	0.0000
	4	0.0001	0.0015	0.0007	0.9945	0.0000	0.0007
	5	0.0004	0.0003	0.0008	0.0002	0.9853	0.0100
	6	0.0001	0.0011	0.0002	0.0001	0.0089	0.9877

* $MAC(i,j) = \frac{(\mathbf{r}_i^T \mathbf{M} \hat{\mathbf{r}}_j)^2}{(\mathbf{r}_i^T \mathbf{M} \mathbf{r}_i)(\hat{\mathbf{r}}_j^T \mathbf{M} \hat{\mathbf{r}}_j)}$, $\mathbf{r}_i$= analytical, and $\hat{\mathbf{r}}_j$= experimental

Table 3: MAC values between analytical and experimental Ritz vectors (using the flexibility based method)

$MAC(i,j)^*$		$\hat{\mathbf{r}}_j$ 1	2	3	4	5	6
$\mathbf{r}_i$	1	0.9992	0.0000	0.0000	0.0000	0.0004	0.0001
	2	0.0000	0.9961	0.0000	0.0021	0.0002	0.0014
	3	0.0000	0.0000	0.9970	0.0007	0.0000	0.0000
	4	0.0000	0.0023	0.0009	0.9941	0.0002	0.0011
	5	0.0004	0.0004	0.0003	0.0007	0.9859	0.0095
	6	0.0002	0.0010	0.0001	0.0002	0.0087	0.9877

* $MAC(i,j) = \frac{(\mathbf{r}_i^T \mathbf{M} \hat{\mathbf{r}}_j)^2}{(\mathbf{r}_i^T \mathbf{M} \mathbf{r}_i)(\hat{\mathbf{r}}_j^T \mathbf{M} \hat{\mathbf{r}}_j)}$, $\mathbf{r}_i$= analytical, and $\hat{\mathbf{r}}_j$= experimental

Table 4: MAC values for different load patterns

Load Point	i for $MAC(i,i)^*$ 1	2	3	4	5	6
NODE 2	0.9958	0.9947	0.9963	0.9969	0.9902	0.9924
NODE 3	0.9985	0.9972	0.9963	0.9954	0.9417	0.9553
NODE 4	0.9993	0.9973	0.9978	0.9928	0.9904	0.9971
NODE 5	0.9993	0.9966	0.9960	0.9958	0.9806	0.9851
NODE 6	0.9989	0.9968	0.9977	0.9967	0.9788	0.9884
NODE 7	0.9951	0.9950	0.9930	0.9906	0.9694	0.9832
NODE 10	0.9929	0.9920	0.9948	0.9918	0.9754	0.9798
NODE 11	0.9979	0.9949	0.9980	0.9969	0.9798	0.9827
NODE 12	0.9994	0.9959	0.9987	0.9976	0.9899	0.9919
NODE 13	0.9997	0.9968	0.9989	0.9956	0.9940	0.9888
NODE 14	0.9994	0.9972	0.9963	0.9967	0.9593	0.9661
NODE 15	0.9969	0.9957	0.9943	0.9986	0.9842	0.9904

* $MAC(i,i) = \frac{(\mathbf{r}_i^T \mathbf{M}\hat{\mathbf{r}}_i)^2}{(\mathbf{r}_i^T \mathbf{M}\mathbf{r}_i)(\hat{\mathbf{r}}_i^T \mathbf{M}\hat{\mathbf{r}}_i)}$, $\mathbf{r}_i$= analytical, and $\hat{\mathbf{r}}_i$= experimental

Table 5: MAC values between analytical and experimental Ritz vectors (with point loads at nodes 2 and 13)

$MAC(i,j)^*$		$\hat{\mathbf{r}}_j$ 1	2	3	4	5	6
$\mathbf{r}_i$	1	0.9992	0.0000	0.0000	0.0000	0.0004	0.0001
	2	0.0000	0.9961	0.0000	0.0021	0.0002	0.0014
	3	0.0000	0.0000	0.9970	0.0007	0.0000	0.0000
	4	0.0000	0.0023	0.0009	0.9941	0.0002	0.0011
	5	0.0004	0.0004	0.0003	0.0007	0.9859	0.0095
	6	0.0002	0.0010	0.0001	0.0002	0.0087	0.9877

* $MAC(i,j) = \frac{(\mathbf{r}_i^T \mathbf{M}\hat{\mathbf{r}}_j)^2}{(\mathbf{r}_i^T \mathbf{M}\mathbf{r}_i)(\hat{\mathbf{r}}_j^T \mathbf{M}\hat{\mathbf{r}}_j)}$, $\mathbf{r}_i$= analytical, and $\hat{\mathbf{r}}_j$= experimental

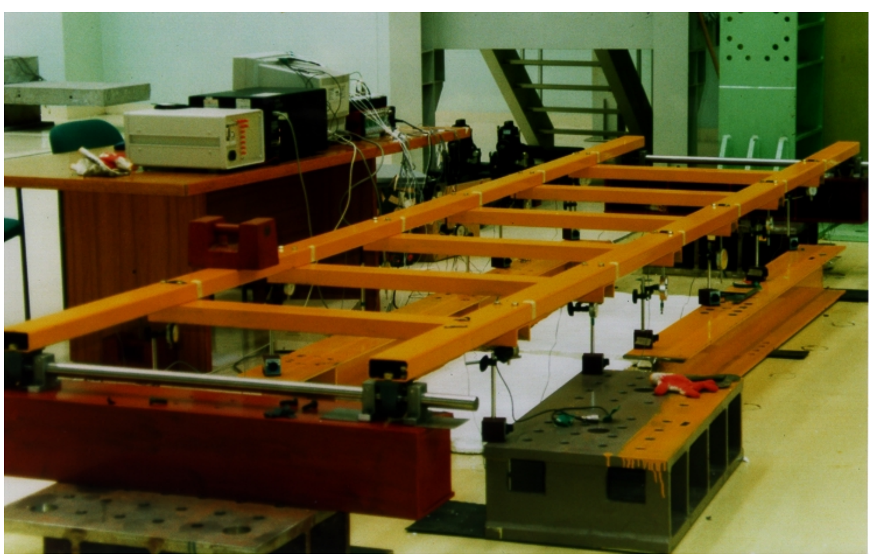

Figure 1: An overview of a grid-type bridge structure

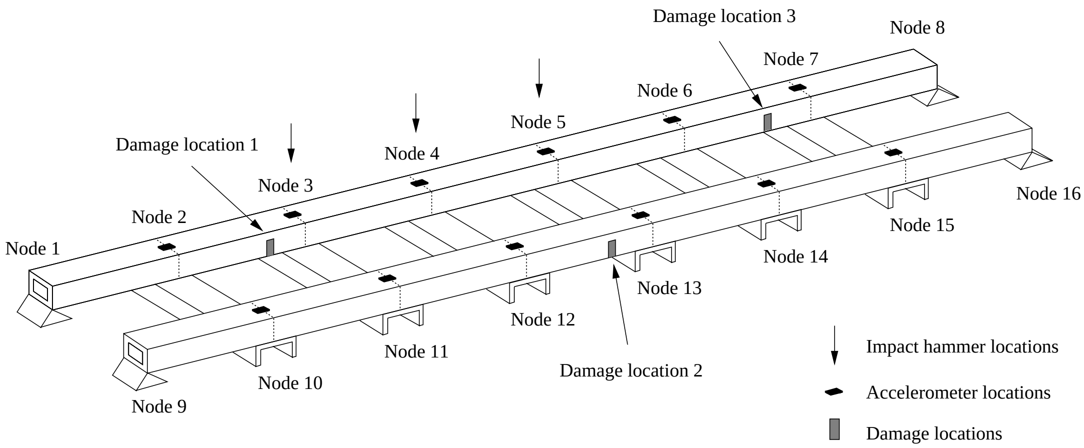

Figure 2: Configuration of a grid-type bridge model

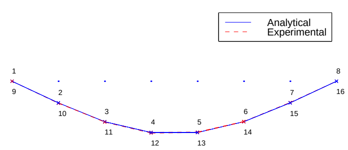

(a) Mode 1

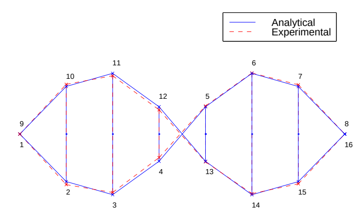

(d) Mode 4

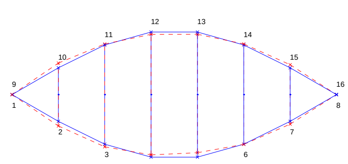

(b) Mode 2

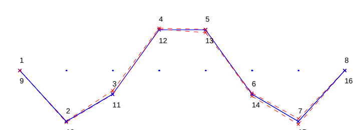

(e) Mode 5

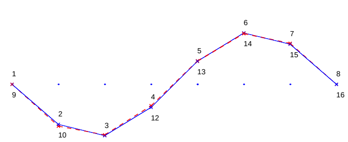

(c) Mode 3

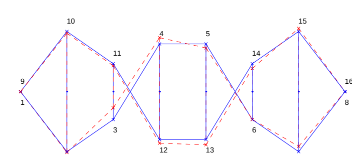

(f) Mode 6

Figure 3: Analytial & experimental modal vectors

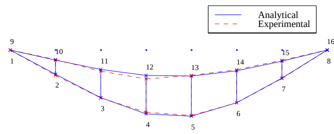

(a) Ritz Vector 1

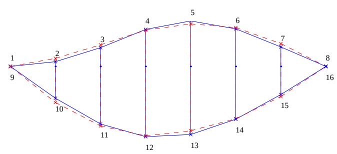

(b) Ritz Vector 2

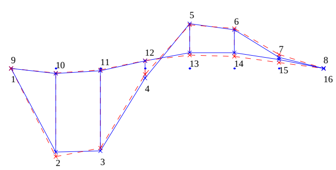

(c) Ritz Vector 3

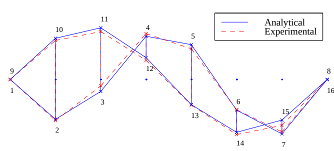

(d) Ritz Vector 4

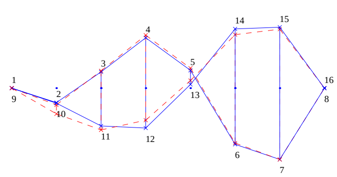

(e) Ritz Vector 5

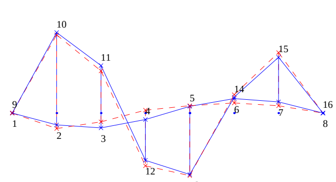

(f) Ritz Vector 6

Figure 4: Comparison of analytical and experimental Ritz vectors (using the state-space based technique)

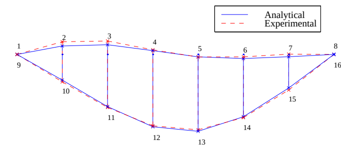

(a) Ritz Vector 1

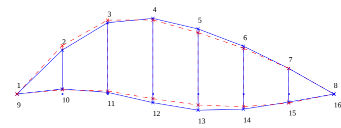

(b) Ritz Vector 2

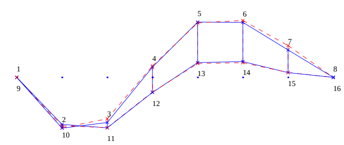

(c) Ritz Vector 3

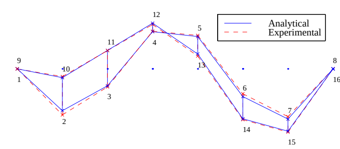

(d) Ritz Vector 4

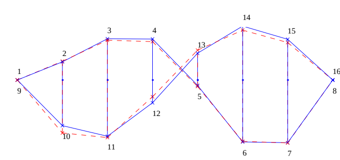

(e) Ritz Vector 5

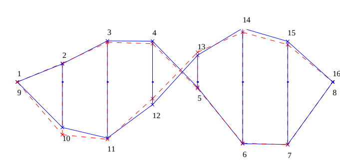

(f) Ritz Vector 6

Figure 5: Experimental Ritz vectors with loading at nodes 2 and 13 (using flexibility based technique)